Distributions of Therapeutically Promising Steroids in Cellular Membranes

Kamila Riedlová,[1,2] Michaela Nekardová [1,3], Petr Kačer,[4] Kamila Syslová,[4] Mario Vazdar,[5]

Pavel Jungwirth,[1,6] Eva Kudová,[1] Lukasz Cwiklik[7*]*

[1]Institute of Organic Chemistry and Biochemistry, Academy of Sciences of the Czech

Republic, Flemingovo nam. 2, 16610 Prague 6, Czech Republic

[2]Faculty of Science, Charles University in Prague, Viničná 5, 128 44 Prague 2, Czech
Republic

[3]Faculty of Mathematics and Physics, Charles University in Prague, Ke Karlovu 3, Prague 2,
121 16, Czech Republic

[4]University of Chemistry and Technology, Technicka 5, 16610 Prague 6, Czech Republic

[5]Rudjer Bošković Institute, Division of Organic Chemistry and Biochemistry, POB 180, HR-

10002 Zagreb, Croatia

[6]Department of Physics, Tampere University of Technology, P. O. Box 692, FI-33101

Tampere, Finland

[7]J. Heyrovský Institute of Physical Chemistry, Academy of Sciences of the Czech Republic,

Dolejškova 3, 182 23 Prague, Czech Republic

[*]*corresponding authors: kudova@uochb.cas.cz (E.K.) and lukasz.cwiklik@uochb.cas.cz*

(L.C.)

Abstract

Interactions of two neurosteroids, inhibiting membrane-bound *N*-Methyl-D-aspartate

receptors, with phospholipid membranes are studied. Namely, endogenous pregnanolone

sulfate is compared with pregnanolone glutamate, the latter being a novel synthetic steroidal inhibitor of these receptors with potential pharmaceutical use. Molecular-level details of steroid-phospholipid membranes interactions are scrutinized employing molecular dynamics simulations supported by quantum chemical calculations to assess steroid lipophilicity. Moreover, permeability of both species across membranes is experimentally evaluated by immobilized artificial membrane chromatography. We demonstrate that while there is no significant difference of lipophilicity and membrane permeability between the two sterols, they differ significantly regarding detailed localization in phospholipid membranes. The bulky glutamate moiety of pregnanolone glutamate is flexible and well exposed to the water phase while the sulfate group of pregnanolone sulfate is hidden in the membrane headgroup region. This dissimilarity of behavior in membranes can potentially account for the observed different activities of the two sterols toward membrane-bound *N*-Methyl-D-aspartate receptors.

Keywords

steroids; *N*-Methyl-D-aspartate receptors; membranes; molecular dynamics; chromatography

Introduction

NMDARs (*N*-Methyl-D-aspartate receptors) belong to a family of glutamate-gated ion channels that play a crucial role in excitatory synaptic transmission (Citri and Malenka, 2008). The overactivation of NMDARs results in excitotoxicity which leads to a specific form of neural cell death. This process is thought to underlie various forms of neurodegeneration, such as Alzheimer disease, ischemia, or traumatic brain injury (Doble, 1999; Mota et al., 2014; Rotaru et al., 2011; Zhou et al., 2013). The activity of NMDARs can be affected by various

allosteric modulators, including neuroactive steroids compounds that are synthetized in the nervous tissue from cholesterol or steroidal precursors from peripheral sources (Baulieu, 1998; Korinek et al., 2011).
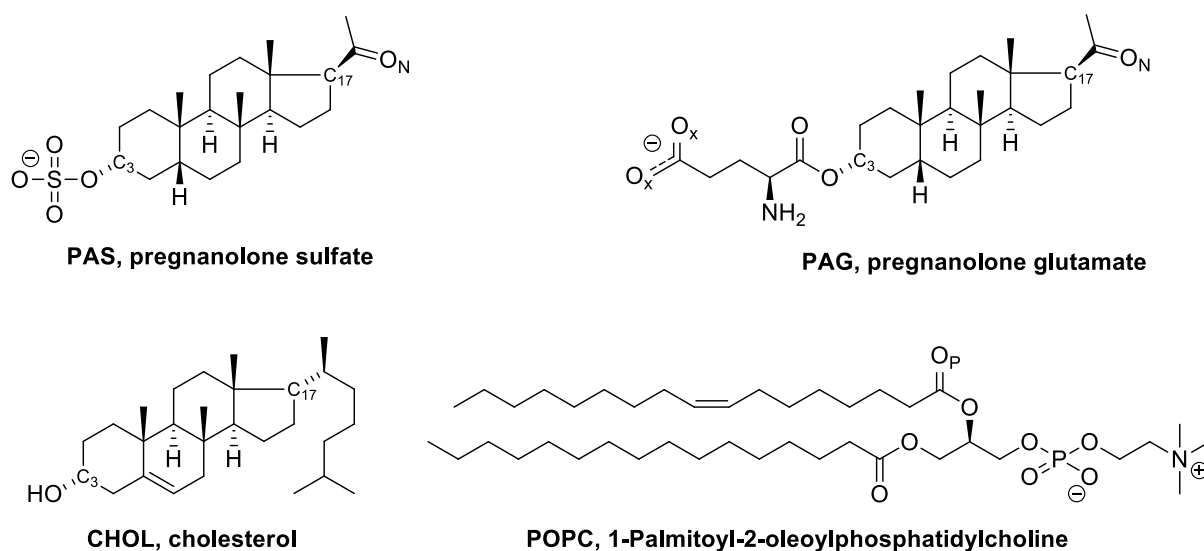
Fig. 1. Structures of pregnanolone sulfate, pregnanolone glutamate, cholesterol and POPC (steroid numbering and subscript indices are used to identify essential atoms).

One of the endogenous neurosteroids that inhibits responses of NMDARs is pregnanolone sulfate (PAS, see Fig. 1) (Petrovic et al., 2005). Neurosteroids are found in the nervous system as free unconjugated steroids, sulfate esters, or fatty acids esters (Jo et al., 1989). However, the sulfate moiety of steroids can undergo hydrolysis by sulfatases that are distributed in various tissues throughout the body (Miki et al., 2002), including the brain tissue (Iwamori et al., 1976). The inhibitory effect of neurosteroids on NMDARs is dependent upon the bent steroid ring structure that is associated with the 5β-stereochemistry and the equatorial C-3 bond. Our previous study on the structure-activity relationship of PAS analogues demonstrated that the C-3 substituent can vary in the length of the linker between

3

the steroid core and the negative charge while maintaining the inhibitory effect on NMDARs (Borovska et al., 2012). Therefore, we have prepared a synthetic NMDAR antagonist – pregnanolone glutamate (PAG, see Fig. 1), derived from naturally occurring pregnanolone sulfate as a novel synthetic steroidal inhibitor of the NMDARs. However, PAS was established (Borovska et al., 2012) as a more potent inhibitor of NMDA-induced currents (IC_{50} = 24.6 μM) than PAG (IC_{50} = 73.4 μM). Nevertheless, our *in vivo* results clearly show that PAG is able to cross the blood brain barrier, does not induce psychotomimetic symptoms (such as hyperlocomotion and sensorimotor gating deficit), and has the desired neuroprotective effect in various biological models (Holubova et al., 2014; Kleteckova et al., 2014; Rambousek et al., 2011). As such, this novel analogue is a promising candidate for further preclinical screening of various indications connected with NMDA-induced excitotoxicity diseases. From this we conclude that the modulatory effect of PAG is a complex process consisting of several factors eventually leading to a strong biological effect. As such, identification of the possible mechanism of PAG action at a molecular level could significantly contribute to NMDA inhibitor pharmacophore definition.

The interactions of neurosteroids with NMDAR constitute a complicated process. It was suggested that neurosteroids form micelles occurring in the extracellular liquid which can fuse with the membrane; next single steroid molecules leave the membrane and enter into the channel vestibule, which is the hydrophobic site of action (Vyklicky et al., 2015). The inhibitors interact with the non-polar NMDAR channel mostly through attractive van der Waals interactions which compete with repulsive effects such as dessolvation and repulsion due to the presence of charged and polar groups in neurosteroids (Barratt et al., 2006).

The kinetics of neurosteroid binding and inhibition is slow and not typical of a simple receptor-ligand interaction in an aqueous solution (Borovska et al., 2012). This indirectly suggests the importance of the plasma membrane as a compartment where the steroid

4

accumulates to reach its site of action on NMDARs. Therefore, examination of the neurosteroid molecules behavior in the membrane using molecular dynamics simulations may clarify their mechanism of action and lead to practical outcomes in the design of new neurosteroids analogues.

In the present study, we have studied the behavior of PAS and PAG molecules in models of the plasma membrane. First, we have focused on the evaluation of physicochemical properties of PAS and PAG employing quantum chemical calculations. Note that the interrelationship of the physicochemical properties and drug absorption/cell penetration is the limiting factor in drug disposition properties (such as absorption, distribution, metabolism, and excretion). As such, the knowledge of physicochemical properties that affect the behavior of the drug in the plasma membrane is essential for further lead optimization and identification phase of the drug discovery process. Second, we used atomistic molecular dynamic simulations of PAS and PAG in both POPC and POPC+cholesterol membranes to gain a molecular-level insight into the properties of the investigated steroids in lipid bilayers, primarily in terms of their localization and orientation. As interactions of the steroids with NMDAR are complex and the proposed mechanism suggests involvement of their lipid bilayer-bound form, it seems crucial to characterize their behavior in lipid membranes. Third, we have experimentally assessed biological properties of PAS and PAG using the immobilized artificial membrane (IAM) chromatography on a IAM.PC.DD2 column which mimics the *in vivo* environment of the plasma membrane (Lázaro et al., 2006; Ledbetter et al., 2012). The IAM method shows a close similarity to human skin partition, tadpole narcosis, and blood-brain permeability processes, hence it is useful as a model of these biological phenomena (Lázaro et al., 2006). By simultaneously employing the three methods which probe length scales ranging from molecular to macroscopic ones, we have gained a comprehensive picture of the behavior of the investigated neuroactive steroids in model lipid membranes.

Methodology

Quantum Mechanics Calculations

Preparation of structures. The structures of the steroids were obtained by the modeling of the molecule taken from the crystal structure (PDBID: 3CAV) (Faucher et al., 2008) using PyMOL program) (Schrodinger, 2015) and were optimized by the RI-DFT/B-LYP/SVP method with Turbomole program (version 6.1) (Ahlrichs et al., 1989). The empirical dispersion correction (D)(Jurečka et al., 2007) and COSMO continuum solvation model (Klamt and Schüürmann, 1993) were employed on the gradient optimization. The most stable local minima of the compounds were generated by the quenched molecular dynamics simulation with PM6-D3H4X (the simulation was run 30 ns; the constant temperature was 350 K) (Rˇezác et al., 2009; Řezáč and Hobza, 2011). The resulting geometries were re-optimized by the RI-DFT-D/B-LYP/SVP/COSMO method and their single-point energies were calculated at the RI-DFT-D3/B-LYP/TZVPP/COSMO level (Grimme et al., 2010).

Estimation of thermodynamic properties. The solvation free energy (ΔG_{solv}) of the compounds was calculated in the SMD continuum solvation model (Marenich et al., 2009) (the transfer from vacuum to water and from *n*-octanol to water for the charged and neutral systems) at the HF/6-31G* level (as recommended in Ref. (Marenich et al., 2009)) with the Gaussian program (version 09) (Frisch et al., 2009).

The partition coefficient is defined as the ratio of concentrations of a neutral solute in *n*-octanol and water, and it represents the solute lipophilicity. It is usually reported as common logarithm:

$$\log P = \log(c_{n,\text{octanol}} / c_{n,\text{water}})$$

The calculated logP (CLogP) was expressed *via* equation $logP = \frac{\Delta G_{ow}}{-RTln(10)}$ (Kolář et al., 2013) where ΔG_{ow} is transfer free energy, R is molar gas constant and T is temperature (298, 15 K). ΔG_{ow} was calculated as the difference between the total energies taken from the optimization of the molecular geometries at the M06-2X/6-31G* level in the SMD continuum aqueous and *n*-octanol environments.

Note that the ΔG_{solv} values are calculated as the single point energies for the same molecular geometries in the two solvents, while ΔG_{ow} calculations take into account the change of geometry related to the transfer between *n*-octanol and water because the resulting total energies include the internal energy of the molecule (Bannan et al., 2016; Kolář et al., 2013). The logarithm of the distribution coefficient:

$$\log D = \log((c_{ion,\text{octanol}} + c_{n,\text{octanol}})/(c_{ion,\text{water}} + c_{n,\text{water}}))$$

which takes into account both neutral and ionized form of the solute in both phases and is used for estimation of lipophilicity of ionizable species (Kah and Brown, 2008) was estimated employing the MarvinSketch software at pH = 7.4 which is the physiological pH of blood serum (ChemAxon, 2015). Experimental IC_{50} values were obtained from literature (Borovska et al., 2012). The maximal inhibitory concentration describes an effectiveness of the steroid in inhibiting a NMDA-induced currents by half.

Electrostatic potential. The electrostatic potentials (ESP) of the steroids were calculated at the HF/cc-pVTZ level. The isodensity surface was mapped with resolution of 0.001 a.u. The images were created by Molekel code (Portmann and Lüthi, 2000).

HPLC-UV Chromatography of Immobilized Model Membranes

PAS and PAG were prepared according to the literature (Borovska et al., 2012). The HPLC Dionex Ultimate 3000 system consisted of a quarter pump, autosampler and Diode Array

Detector (DAD) (Thermo Scientific, USA). The mobile phase consisted of methanol (A) and a DPBS solution in deionized water (pH 5.4), DPBS solution consisting of calcium chloride (0.9 mM), potassium chloride (2.67 mM), potassium phosphate monobasic (1.47 mM), magnesium chloride (0.6 mM), sodium chloride (138 mM) and Sodium Phosphate Dibasic (8.1 mM) (B). Prior to using the mobile phase, it was degassed one hour with vacuum and filtered through a 0.22 μm nylon membrane (Millipore Co., Milford, MA). The mobile phase was delivered at the flow rate of 1.0 ml.min^{-1}. The compounds were isocratically eluted (70 % B) on IAM.PC.DD2 on 10 μm (particle size), 150 mm × 4.6 mm stainless steel column (Regis, USA) with an immobilized artificial membrane and then detected at 254 nm. The chromatographic analysis was performed at 37 °C. The injection volume was 10 μl. Data were acquired and evaluated using Chromeleon™ 7.1 Chromatography Data System (CDS) software.

MD Simulations

Classical molecular dynamics simulations were applied to study the behavior of PAG or PAS molecules in lipid bilayers formed of either pure POPC or POPC with 28.9 mol% of cholesterol. Simulations were performed employing the GROMACS 4.6.1 software package (Hess et al., 2008). The systems for molecular dynamics simulation consisted of 128 POPC molecules with 64 lipid molecules in each leaflet. In the case of the cholesterol-containing bilayer, additional 52 cholesterol molecules were added to the membrane (26 in each leaflet). The bilayers were hydrated with approximately 6000 molecules of water to obtain the water to lipids ratio of over 45. The bilayers were built based on previously equilibrated systems and here they were further equilibrated for 20 ns. Both Na$^+$ and Cl$^-$ ions were added to the water phase in the amount resulting in 150 mM salt concentration. Additional sodium cations were added to neutralize the negative charge of PAG or PAS. The resulting total number of Na$^+$ in the simulation box was 23 whereas that of Cl$^-$ was 15. Eight molecules of either PAG

8

or PAS were added to the bilayers (these numbers correspond to 6 and 4 mol% of steroid in cholesterol-free and cholesterol-containing POPC bilayers, accordingly). More specifically, the insertion of steroids was realized by employing the standard pulling method of GROMACS. Two possible orientations of steroids in membrane were tested. Namely, steroids were pulled into the membranes with their charged groups directed toward either the lipid-water interface or the membrane core. In the latter case, steroids were not stable in the bilayers (they either desorbed or reoriented) hence only the membranes with steroids oriented with their headgroups toward the water phase were used for further simulations. Upon insertion of steroids, each system was simulated for 200 ns and the last 100 ns of trajectories were used for analysis.

Lipid molecules were modeled by using the Berger's united-atom force field (Berger et al., 1997) while water molecules were described with the SPC model for which Berger's parameterization was derived (Berendsen et al., 1981). Parameters for ions were taken from the GROMACS force field (Hess et al., 2008). The Holtje and co-workers force filed was employed for cholesterol (Höltje et al., 2001). Parameters for both PAG and PAS molecules were derived based on the cholesterol parameterization with missing terms taken from the GROMACS force field. Both PAG and PAS were modelled in their anionic forms in which they predominantly occur in water, as well as in the hydrophilic headgroup region of the bilayer (see Fig. 1). Partial charges were obtained with the RESP method based on quantum calculation at the density functional theory level employing the B3LYP functional and the 6-31g(d) basis set (Cornell et al., 1993; Stephens et al., 1994). These calculations were performed using the Gaussian code (Frisch et al., 2009). The derived force field parameters are given in the Supplementary Material.

Simulations were carried out employing the isothermal-isobaric ensemble with the pressure of 1 bar controlled in the semi-isotropic setup by the Parinello-Rahman algorithm

with the time constant of 2 ps (Parrinello and Rahman, 1981). The temperature of 310 K was controlled by the Nose-Hoover thermostat algorithm with the time constant of 1 ps (Nose, 1984). The geometry of water molecules was restricted employing the SETTLE method (Hockney et al., 1974) while bond lengths of lipids were kept constant employing the LINCS algorithm (Hess et al., 1997). Equations of motions were integrated with the 2 fs time step during PAS simulations. In the case of PAG, the time step of 0.5 fs was employed in order to avoid instabilities during the solution of the equations of motion. The simulation box had an approximate size of $6\times6\times9$ nm^3. The periodic boundary conditions were applied. The cut-off of 1 nm was employed for both non-bonded interactions and short-range electrostatic interactions. The long-range electrostatic interactions were accounted for employing the particle-mesh Ewald method (Essmann et al., 1995). The details regarding analysis of atomic contacts are given in the Supplementary Material. Visualization of MD trajectories was performed employing the VMD software (Humphrey et al., 1996).

Results and Discussion

Physicochemical Properties of PAS and PAG from Quantum Chemical Calculations

Lipophilicity belongs to basic characteristics of neurosteroids and influences their interactions with NMDAR (Kudova et al., 2015). The physicochemical properties that characterize lipophilicity of PAS and PAG as estimated by quantum chemical computational methods (ΔG_{solv} and logP) and by physicochemical properties predictor (logD) are given in Table 1 together with experimentally (Borovska et al., 2012) estimated values of IC$_{50}$.Note that for both compounds, IC$_{50}$ is in the range of tens of μmol/l with PAS exhibiting a stronger inhibitory effect than PAG. The solvation free energy ΔG_{solv} was calculated for transfer of a single neurosteroid molecule from vacuum to aqueous solution, as well as from *n*-octanol

(which is a model of a membrane environment) to an aqueous solution. The calculated values of ΔG_{solv} indicate that both steroids are water-soluble as there is free energy gain during their transfer from vacuum to water; with the charged forms being more stable in water than the neutral ones. Regarding the octanol-water transfer, neutral forms slightly prefer the octanol phase, while charged forms exhibit a free energy gain when transferred to water. Relatively small free energy values indicate that the transfer between octanol and water phases is possible and it would be accompanied by the change of the ionization state. Note that the relative values of ΔG_{solv} may to some extent be influenced by conformational changes during the transfer because the substituent at C3 of PAG molecule is more flexible than that sulfate moiety in PAS. Overall, the differences of calculated ΔG_{solv} between PAS and PAG are relatively small.

Table 1. Physicochemical properties of PAS and PAG. The negative values of ΔG_{solv} signify the free energy gain, and the positive values signify the free energy required during the transfer from the first phase to the second phase (*n*-octanol represents the membrane environment). Experimentally measured values of IC_{50} are given in the first column.

Steroid	IC_{50} [μmol/l]	ΔG_{solv} [kcal/mol] (SMD) - transfer:				logP	logD
		from vacuum to water		from *n*-octanol to water			
		neutral	charged	neutral	charged		
PAS	24.60	-20.90	-75.18	1.83	-5.53	2.93	1.67
PAG	73.40	-31.46	-88.94	1.48	-6.38	3.09	1.21

The lipophilic character of the PAS and PAG molecules was also estimated via the logP and logD coefficients. Note that these two quantities are often employed in pharmacological studies of drug-like compounds and the higher logP and logD values are, the higher

lipophilicity is. The value of logP estimates lipophilicity of a molecule including lipophilic contributions of both the parent molecule and its substituents (Faassen et al., 2003). As both PAS and PAG can be ionized or neutral depending on the pH, exhibiting different polarities, the distribution coefficient logD should be a better estimate of lipophilicity (Kah and Brown, 2008). The calculated logP and logD demonstrate that lipophilicity of PAS and PAG is similar, in accord with the ΔG_{solv}.

We have estimated electrostatic potentials (ESP) for PAS and PAG (see Fig. 2). The electron distribution suggests that both steroids would have a tendency to attain a preferred orientation in the membrane environment. The PAS sulfate group and the PAG carboxyl group carry the strong negative charged areas, while the cores of the molecules have significantly less negative charge. On the basis of ESP maps we can assume that both functional groups are situated at the level of the hydrated phosphate heads. This is in accord with results of MD simulations, which clearly show the preferred positions of the molecules in the membrane (*vide infra*).
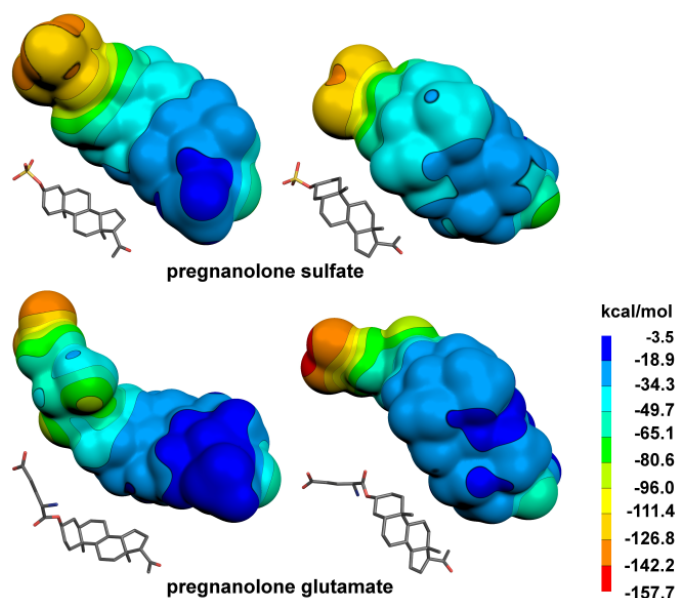
Fig. 2. Electrostatic potentials of representative, low-energy gas-phase conformations of considered steroids.

Chromatography of Immobilized Model Membranes

The stationary phase of IAM.PC.DD2 column is prepared from phosphatidylcholine analogues that are bound to monolayer of silica particles (see Fig. 3). As the POPC is the major phospholipid in the cell membrane, the chromatography can mimic the surface of a biological membrane. Also, this technique offers an alternative approach to traditional description of logarithm of octanol-water partition coefficient (logP) to determination of hydrophobicity (Lázaro et al., 2006; Ledbetter et al., 2012).
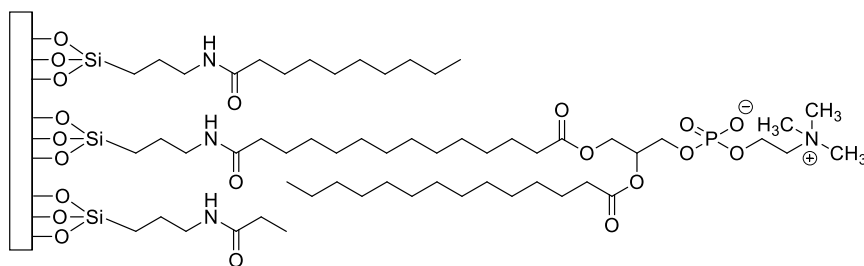
Fig. 3. Structure of the IAM.PC.DD2 stationary phase employed in the chromatography of immobilized model membranes.

Table 2. Experimentally measured values of retention factor K_{IAM} of PAS and PAG, Molecular weight and computationally estimated logP and logD values are also given.

Steroid	K_{IAM}	MW	logP	logD
Pregnanolone sulfate (PAS)	42.0	398.55	2.93	1.67
Pregnanolone glutamate (PAG)	43.0	447.60	3.09	1.21

The permeability of PAS and PAG was characterized by the retention factor K_{IAM} using a methanol/PBS mobile phase (for details see Experimental Section). The results are summarized in Table 2. The equation for K_{IAM} calculation can be expressed as:

$$K_{IAM} = (t_r - t_0)/t_0$$

The results show that the retention factors K_{IAM} of PAS and PAG on artificial membrane are comparable which is in agreement with the ~1.12-fold difference of their molecular weight (for detailed method description and validation see Supplementary Material). These data suggest that the differences between interactions of PAS and PAG with NMDARs observed *in vivo* cannot be assigned exclusively to their physicochemical permeability across the membrane.

Note that we employ the solubility-diffusion model, usually used in pharmaceutical studies which assumes that the crossing of the membrane is predominantly controlled by partitioning of a molecule in the lipid bilayer (Finkelstein, 1976). Such an approach is justified when the diffusivity differences of the considered molecules are relatively minor in the membrane. We make such an assumption as the size and chemical structure of both steroids is similar.

Localization and orientation of PAS and PAD in model membranes – MD Simulations

Typical snapshots of the equilibrated systems with either PAS or PAG molecules in cholesterol-free and cholesterol-containing POPC bilayers obtained during MD simulations are depicted in Fig. 4. Qualitatively, in each simulated system steroid molecules incorporate in the lipid bilayer residing between lipid molecules. Their charged groups locate predominantly in the relatively well hydrated lipid headgroup region whereas their ring

systems occupy the dehydrated hydrocarbon membrane core. In the case of cholesterol-free membranes (Figs. 4A and 4C), orientation of steroid molecules is more flexible than that in membranes with cholesterol (Figs. 4B and 4D). In the latter membranes, both PAS and PAG reside in the same region as cholesterol molecules.
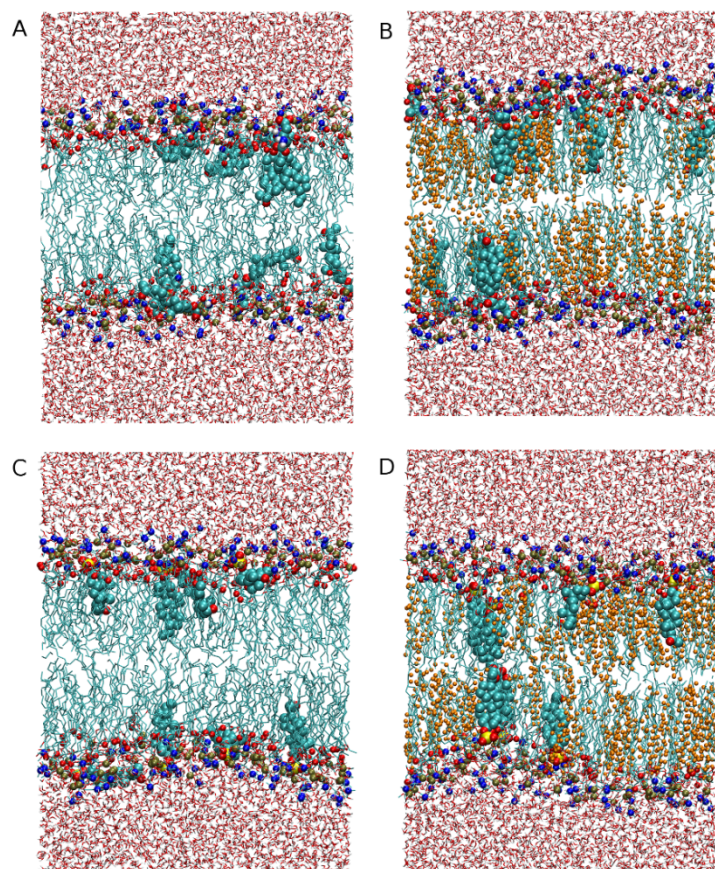
Fig. 4. Typical snapshots depicting simulation boxes of the systems containing PAS in POPC bilayer (A), PAS in POPC+cholesterol bilayer (B), PAG in POPC bilayer (C), and PAG in POPC+cholesterol bilayer (D). Side-view of the boxes are presented with the following color coding: water – red and white points, nitrogen in choline of POPC – navy blue balls, phosphorus of POPC phosphates – gold balls, carbonyl oxygen of POPC and sterols – red balls, acyl chains of POPC – blue lines, carbon atoms of sterols – blue balls.
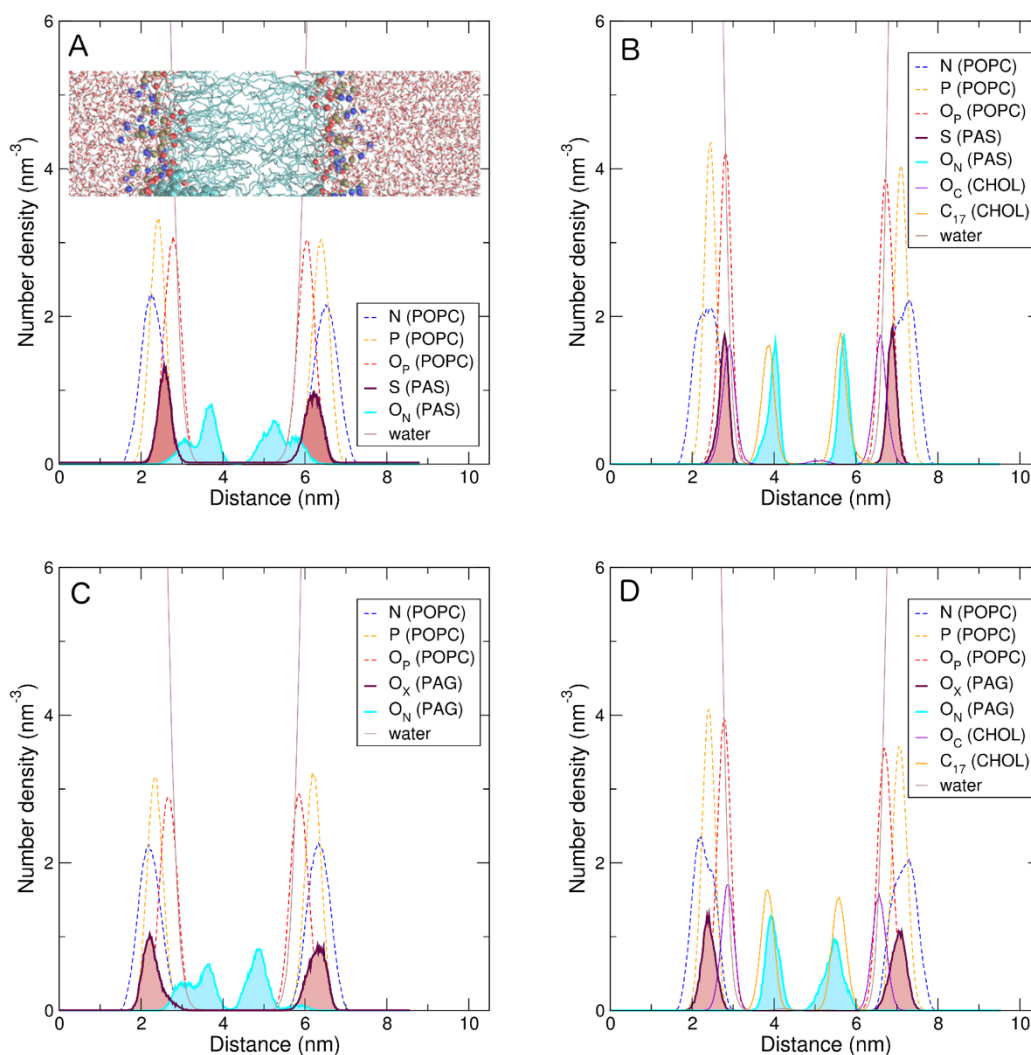
Fig. 5. Density profiles of selected system components calculated along the bilayer normal in the equilibrated section of the MD trajectories for PAS in POPC (A), PAS in POPC+cholesterol (B), PAG in POPC (C), and PAG in POPC+cholesterol (D). Note that the density profiles in both membrane leaflets are shown in graphs. In the background of the subfigure (A), a schematic view of a fragment of the simulation box corresponding to the density profiles was shown (with the same color coding as in Fig. 4). The profiles of atoms in glutamate and sulfate moieties of PAG and PAS as well as these of O_N atoms of both steroids were filled with color for clarity of presentation. See Fig. 1 for definition of atom names.

The density profiles depicted in Fig. 5 enable a quantitative analysis of steroids localization in the considered bilayers. In the case of PAS in POPC (Fig. 5A), the S atom of

the charged SO_3^- moiety resides exclusively in the polar region (occupied by choline, phosphate, and sn-2 carbonyl groups) of the POPC bilayer as evidenced by the unimodal S densities in both leaflets. In contrast, the density profile of the oxygen atom O_N of PAS is bimodal in each membrane leaflet (see Fig. 1 for definition of atom names). This is due to two possible localizations of the O_N atom in POPC bilayer. Namely, O_N resides either in the hydrocarbon membrane core (the peaks at 3.8 and 5.2 nm) or in the hydrated region overlapping with that of carbonyl O_P atoms of POPC (the peaks at 3.0 and 5.8 nm). This bimodality is related to two possible orientations of the PAS molecule in the POPC membrane. More specifically, PAS is either located predominantly in parallel to the POPC chains ('vertical' orientation) or it attains configurations in which its polar O_N side penetrates toward the hydrated region of the membrane leading to PAS molecule oriented in parallel to the lipid-water interface ('horizontal' orientation). These two possible orientations are also evidenced in the snapshot in Fig. 4A.

In the case of PAS in the POPC+cholesterol membrane (Fig. 5B), there is one key difference with regard to the cholesterol-free case. Specifically, the O_N density profile is unimodal in each leaflet which is because of only one possible orientation ("vertical") of PAS in the presence of cholesterol (see also Fig. 4B). Hence, the charged SO_3^- group of PAS is oriented toward the lipid-water interface while the polar O_N atom resides exclusively in the dehydrated bilayer core. In this respect, behavior of PAS is similar to that of cholesterol; this is also evident from the very similar density profiles of O_N of PAS and C_{17} of cholesterol as well as those of S of PAS and O_C in cholesterol. The loss of orientational flexibility of PAS can be rationalized by membrane rigidification by cholesterol (Róg and Pasenkiewicz-Gierula, 2001).

In terms of density profiles (Fig. 5C), behavior of PAG in the POPC membrane mostly follows that of PAS. Namely, the density profiles of the charged carboxylic group of PAG

overlaps with the profiles of POPC headgroup atoms hence the charged group is exclusively oriented toward the water phase. The O_N atom at the opposite side of the PAG molecule has a bimodal density profile in each leaflet because of the possible 'vertical' and 'horizontal' orientation of PAG in POPC. Note that the O_N density profiles are less similar between both leaflets for PAS (Fig. 4A) than for PAG (Fig. 4C) indicating some difficulty in obtaining statistically fully converged data. This is due to a relatively slow process of reorientation of the bulky PAG in the bilayer during the finite MD simulation time in comparison with reorientation of relatively small PAS. An important difference between PAG and PAS is a better exposure of the relatively bulky glutamic moiety of PAG at the lipid-water interface in comparison with that of PAS. This is visible in position of S (PAS) and O_X (PAG) density profiles with respect to the position of the density profile of N atom in choline group of POPC (compare Figs. 5A and 5C).

In the cholesterol-containing POPC bilayer, PAG molecules loose the 'horizontal' orientation, as evidenced by unimodal O_N density profiles in both leaflets in Fig. 5D. Similarly to PAS, density profiles of O_N atoms of PAG overlap with those of C17 atom of cholesterol. As in the cholesterol-free case, the glutamic moiety of PAG is relatively well exposed at the lipids-water interface.

The two possible orientations of both PAS and PAG in POPC are also evident based on the tilt angle distributions presented in Fig. 6. The distributions in the cholesterol-free bilayers are relatively wide, ranging up to 100°. In the POPC+cholesterol system, the distributions are significantly narrower, up to 30°. The tilt angles below 30° are related to the 'vertical' orientation while it can be assumed that the values between 30 and 90° are responsible for the whole spectrum of different 'horizontal' orientations. Note that neither PAS nor PAG completely reorient in the considered membranes as tilt angles significantly above 90° were not observed in the simulations. Also, based on the tilt angle distributions, the

'vertical' orientation in both PAS and PAG is more populated than the 'horizontal' one as the tilt angles above 30° are relatively weakly populated.
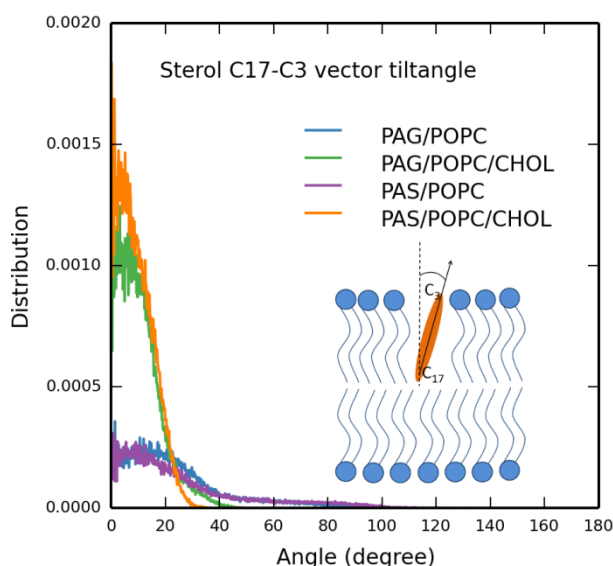
Fig. 6. Distribution of sterol tilt angles (the angle between the C_{17}-C_3 vector in either PAS or PAG with respect to the bilayer normal) calculated in the equilibrated section of the MD trajectories. In the inset, a schematic definition of the tilt angle is given.

Further information regarding atomistic details of steroid orientation in lipid bilayers can be gained from analysis of atomic contacts. In Fig. 7, numbers of contacts between selected atoms in each simulated system are presented. The data in Fig. 7A confirm that PAS in the POPC bilayer has its SO_3^- moiety in contact with phosphate, choline, and *sn-2* carbonyl groups of POPC as well as with water. The contacts of the O_N atom of PAS with both POPC headgroups and water are less pronounced but not negligible, proving the existence of the 'horizontal' orientation of PAS in POPC. In the cholesterol containing membrane (Fig. 7B), O_N of PAS has no contacts with the abovementioned atoms, hence the 'horizontal' orientation does not occur in the presence of cholesterol. Similar trends are present in the case of PAG

(Figs. 7C and 7D), where the O_N atom loses contact with lipid headgroups of POPC. Note also that a better exposition of the glutamic moiety of PAG at the water-lipid interface than that of the SO_3 group of PAS is visible as the number of contact of these groups with water differ almost by one (compare Figs. 7A and 7B with 7C and 7D).
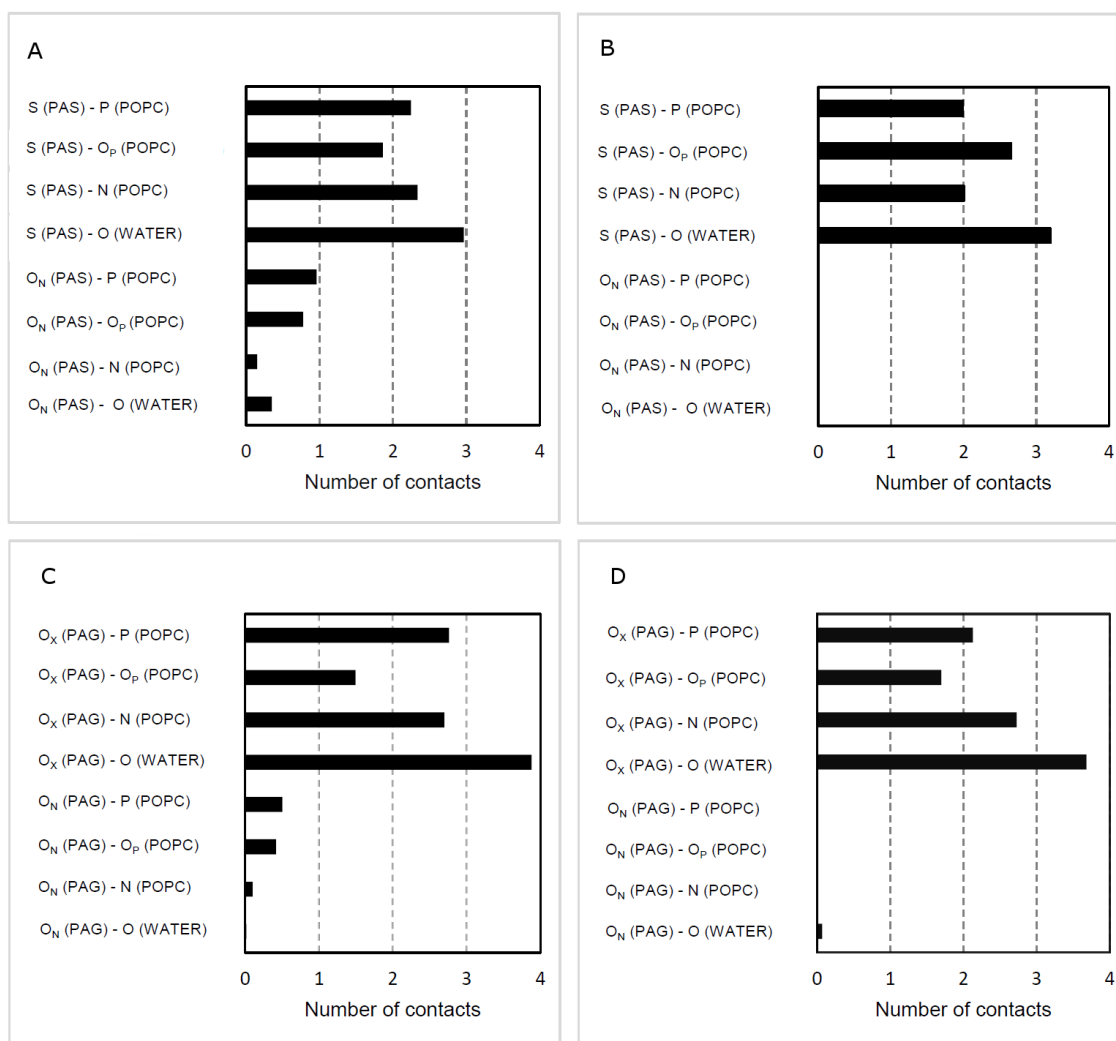
Fig. 7. Numbers of contacts between selected system components calculated in the equilibrated section of the MD trajectories containing PAS in POPC (A), PAS in POPC+cholesterol (B), PAG in POPC (C), and PAG in POPC+cholesterol (D). The distance cutoffs for atomic contacts are given in the Supplementary Material.

Conclusions

The aim of the present work was to characterize interactions of PAS and PAG, two neurosteroids that inhibit *N*-Methyl-D-aspartate receptors, with a model biological membrane. This was motivated by a hypothesis that cellular membranes mediate interactions between neurosteroids and NMDRs. For this purpose, steroid lipophilicity was assessed employing quantum chemical calculations supported by experimental measurements of the steroids partitioning in membranes. These techniques demonstrated that both PAS and PAG exhibit similar propensity to lipid phases.

As demonstrated previously, regarding IC_{50} values, PAS, which is an endogenous neurosteroid that inhibits NMDAR, evinces more than twice as good inhibitory effect as PAG. The lower efficiency of PAG was suggested to be caused by the difference in the structure of the very flexible substituent at C3, while the PAS sulfate group is rather rigid. The difference between IC_{50} values is in contrast to the relatively small differences between estimated lipophilicity of both steroids and the measured membrane partitioning. Note that lipophilicity was shown previously for sulfated neurosteroids bearing nonpolar modification on the D-ring (e.g. methyl, ethyl, butyl, etc.) to be closely related to their inhibitory effect (Kudova et al., 2015).

The molecular-level insight obtained via MD simulations let us to resolve these issues. MD simulations demonstrate that PAS and PAG are stabilized both in pure POPC and mixed POPC/cholesterol bilayers. The charged groups of the steroids are oriented toward the lipid-water interface while their carbonyl oxygen atoms reside predominantly in the membrane core. In cholesterol-free systems, the carbonyl groups can reorient toward water leading thus to a 'horizontal' orientation of the steroid molecules in lipid membrane. The glutamate moiety

of PAG is relatively well exposed at the lipid-water interface while the SO_3 group of PAS is more buried between POPC headgroups. MD simulations show that both steroids significantly differ concerning their presentation of their polar moieties, glutamate and sulfate, at the membrane-water interface. The bulkier glutamate in PAG is more water-exposed than sulfate in PAS. Similarly, conformational freedom of the glutamate group of PAG is larger than that of sulfate in PAS. Both the different presentation of the polar groups and the diverse conformations of PAG can account for the observed alterations in interaction of PAG and PAS with NMDARs indicated by the different IC_{50} values. Note also that simulations point out that orientation of the considered steroid molecules in phosphatidylcholine membranes can be altered indirectly by varying cholesterol content. The latter can be of importance as cholesterol content differs considerably in various organs and various cell membranes, it can be also precisely controlled in artificial drug delivery systems, which is of potential interest in the pharmacological context.

One should be aware of limitations that the presented model of steroids in membranes has regarding the steroids-NMDARs issue. First, the receptor is not present in the system hence only indirect conclusions about interactions of steroid with a site of action can be made. Second, lipid composition of the membrane is of limited complexity in comparison with actual cell membranes. Third, the protonation state of sterols can, in principle, change while going from well the hydrated water environment to the lipid membrane. All of these issues will be addressed in future research. Despite these weak points, the present simulations let us to identify basic differences in behavior of PAG and PAS in lipid membranes and hence provided a basis for interpretation of the observed differences in inhibition of NMDARs.

Acknowledgements

Supplementary Material

Force field parameters of PAG and PAS. The distance cutoffs for atomic contacts.

The authors declare no competing financial interest.

References

Ahlrichs, R., Bär, M., Häser, M., Horn, H., Kölmel, C., 1989. Electronic structure calculations on workstation computers: The program system turbomole. Chem. Phys. Lett. 162, 165-169.

Bannan, C.C., Calabró, G., Kyu, D.Y., Mobley, D.L., 2016. Calculating partition coefficients of small molecules in octanol/water and cyclohexane/water. Journal of Chemical Theory and Computation 12, 4015-4024.

Barratt, E., Bronowska, A., Vondrášek, J., Černý, J., Bingham, R., Phillips, S., Homans, S.W., 2006. Thermodynamic Penalty Arising from Burial of a Ligand Polar Group Within a Hydrophobic Pocket of a Protein Receptor. Journal of Molecular Biology 362, 994-1003.

Baulieu, E., 1998. Neurosteroids: a novel function of the brain. Psychoneuroendocrinology 23, 963-987.

Berendsen, H.J.C., Postma, J.P.M., Van Gunsteren, W.F., Hermans, J., 1981. Interaction Models for Water in Relation to Protein Hydration, Intermolecular Forces. D. Reidel Publishing Company, Dordrecht, pp. 331–342.

Berger, O., Edholm, O., Jahnig, F., 1997. Molecular dynamics simulations of a fluid bilayer of dipalmitoylphosphatidylcholine at full hydration, constant pressure, and constant temperature. Biophysical Journal 72, 2002-2013.

Borovska, J., Vyklicky, V., Stastna, E., Kapras, V., Slavikova, B., Horak, M., Chodounska, H., Vyklicky Jr, L., 2012. Access of inhibitory neurosteroids to the NMDA receptor. British journal of pharmacology 166, 1069-1083.

ChemAxon, M., 2015. ChemAxon. Ltd.

Citri, A., Malenka, R.C., 2008. Synaptic plasticity: multiple forms, functions, and mechanisms. Neuropsychopharmacology 33, 18-41.

Cornell, W.D., Cieplak, P., Bayly, C.I., Kollmann, P.A., 1993. Application of RESP charges to calculate conformational energies, hydrogen bond energies, and free energies of solvation. J. Am. Chem. Soc. 115, 9620-9631.

Doble, A., 1999. The role of excitotoxicity in neurodegenerative disease: implications for therapy. Pharmacology & therapeutics 81, 163-221.

Essmann, U., Perera, L., Berkowitz, M.L., Darden, T., Lee, H., Pedersen, L.G., 1995. A smooth particle mesh Ewald method. J Chem Phys 103, 8577-8593.

Faassen, F., Kelder, J., Lenders, J., Onderwater, R., Vromans, H., 2003. Physicochemical properties and transport of steroids across Caco-2 cells. Pharmaceutical research 20, 177-186.

Faucher, F.d.r., Cantin, L., Luu-The, V., Labrie, F., Breton, R., 2008. The Crystal Structure of Human Δ4-3-Ketosteroid 5β-Reductase Defines the Functional Role of the Residues of the Catalytic Tetrad in the Steroid Double Bond Reduction Mechanism†. Biochemistry 47, 8261-8270.

Finkelstein, A., 1976. Water and nonelectrolyte permeability of lipid bilayer membranes. The Journal of general physiology 68, 127-135.

Frisch, M., Trucks, G., Schlegel, H.B., Scuseria, G., Robb, M., Cheeseman, J., Scalmani, G., Barone, V., Mennucci, B., Petersson, G., 2009. Gaussian 09, Revision A. 02, Gaussian. Inc., Wallingford, CT 200.

Grimme, S., Antony, J., Ehrlich, S., Krieg, H., 2010. A consistent and accurate ab initio parametrization of density functional dispersion correction (DFT-D) for the 94 elements H-Pu. The Journal of chemical physics 132, 154104.

Hess, B., Bekker, H., Berendsen, H.J.C., Fraaije, J.G.E.M., 1997. LINCS: A linear constraint solver for molecular simulations. J. Comput. Chem. 18, 1463-1472.

Hess, B., Kutzner, C., van der Spoel, D., Lindahl, E., 2008. GROMACS 4: Algorithms for Highly Efficient, Load-Balanced, and Scalable Molecular Simulation. J. Chem. Theory Comput. 4, 435-447.

Hockney, R.W., Goel, S.P., Eastwood, J.W., 1974. Quiet High-Resolution Computer Models of a Plasma. J Comput Phys 14, 148-158.

Höltje, M., Förster, T., Brandt, B., Engels, T., von Rybinski, W., Höltje, H.-D., 2001. Molecular dynamics simulations of stratum corneum lipid models: fatty acids and cholesterol. Biochimica et Biophysica Acta (BBA)-Biomembranes 1511, 156-167.

Holubova, K., Nekovarova, T., Pistovcakova, J., Sulcova, A., Stuchlík, A., Vales, K., 2014. Pregnanolone glutamate, a novel use-dependent NMDA receptor inhibitor, exerts antidepressant-like properties in animal models. Frontiers in behavioral neuroscience 8.

Humphrey, W., Dalke, A., Schulten, K., 1996. VMD: visual molecular dynamics. Journal of molecular graphics 14, 33-38.

Iwamori, M., Moser, H., Kishimoto, Y., 1976. Steroid sulfatase in brain: comparison of sulfohydrolase activities for various steroid sulfates in normal and pathological brains, including the various forms of metachromatic leukodystrophy. Journal of neurochemistry 27, 1389-1395.

Jo, D.-H., Abdallah, M.A., Young, J., Baulieu, E.-E., Robel, P., 1989. Pregnenolone, dehydroepiandrosterone, and their sulfate and fatty acid esters in the rat brain. Steroids 54, 287-297.

Jurečka, P., Černý, J., Hobza, P., Salahub, D.R., 2007. Density functional theory augmented with an empirical dispersion term. Interaction energies and geometries of 80 noncovalent complexes compared with ab initio quantum mechanics calculations. J Comput Chem 28, 555-569.

Kah, M., Brown, C.D., 2008. LogD: Lipophilicity for ionisable compounds. Chemosphere 72, 1401-1408.

Klamt, A., Schüürmann, G., 1993. COSMO: a new approach to dielectric screening in solvents with explicit expressions for the screening energy and its gradient. Journal of the Chemical Society, Perkin Transactions 2, 799-805.

Kleteckova, L., Tsenov, G., Kubova, H., Stuchlik, A., Vales, K., 2014. Neuroprotective effect of the $3\alpha5\beta$-pregnanolone glutamate treatment in the model of focal cerebral ischemia in immature rats. Neuroscience letters 564, 11-15.

Kolář, M., Fanfrlík, J., Lepšík, M., Forti, F., Luque, F.J., Hobza, P., 2013. Assessing the Accuracy and Performance of Implicit Solvent Models for Drug Molecules: Conformational Ensemble Approaches. The Journal of Physical Chemistry B 117, 5950-5962.

Korinek, M., Kapras, V., Vyklicky, V., Adamusova, E., Borovska, J., Vales, K., Stuchlik, A., Horak, M., Chodounska, H., Vyklicky, L., 2011. Neurosteroid modulation of N-methyl-d-aspartate receptors: molecular mechanism and behavioral effects. Steroids 76, 1409-1418.

Kudova, E., Chodounska, H., Slavikova, B., Budesinsky, M., Nekardova, M., Vyklicky, V., Krausova, B., Svehla, P., Vyklicky, L., 2015. A New Class of Potent N-Methyl-d-Aspartate Receptor Inhibitors: Sulfated Neuroactive Steroids with Lipophilic D-Ring Modifications. Journal of medicinal chemistry 58, 5950-5966.

Lázaro, E., Ràfols, C., Abraham, M.H., Rosés, M., 2006. Chromatographic estimation of drug disposition properties by means of immobilized artificial membranes (IAM) and C18 columns. Journal of medicinal chemistry 49, 4861-4870.

Ledbetter, M.R., Gutsell, S., Hodges, G., Madden, J.C., Rowe, P.H., Cronin, M.T., 2012. Robustness of an Immobilized Artificial Membrane High-Performance Liquid Chromatography Method for the Determination of Lipophilicity. Journal of Chemical & Engineering Data 57, 3696-3700.

Marenich, A.V., Cramer, C.J., Truhlar, D.G., 2009. Universal solvation model based on solute electron density and on a continuum model of the solvent defined by the bulk dielectric constant and atomic surface tensions. The Journal of Physical Chemistry B 113, 6378-6396.

Miki, Y., Nakata, T., Suzuki, T., Darnel, A.D., Moriya, T., Kaneko, C., Hidaka, K., Shiotsu, Y., Kusaka, H., Sasano, H., 2002. Systemic distribution of steroid sulfatase and estrogen sulfotransferase in human adult and fetal tissues. The Journal of Clinical Endocrinology & Metabolism 87, 5760-5768.

Mota, S.I., Ferreira, I.L., Rego, A.C., 2014. Dysfunctional synapse in Alzheimer's disease–A focus on NMDA receptors. Neuropharmacology 76, 16-26.

Nose, S., 1984. A molecular dynamics method for simulations in the canonical ensemble. Mol. Phys. 52, 255-268.

Parrinello, M., Rahman, A., 1981. Polymorphic transitions in single crystals: A new molecular dynamics method. Journal of Applied Physics 52, 7182-7190.

Petrovic, M., Sedlacek, M., Horak, M., Chodounska, H., Vyklický, L., 2005. 20-Oxo-5β-pregnan-3α-yl sulfate is a use-dependent NMDA receptor inhibitor. The Journal of neuroscience 25, 8439-8450.

Portmann, S., Lüthi, H.P., 2000. MOLEKEL: an interactive molecular graphics tool. CHIMIA International Journal for Chemistry 54, 766-770.

Rˇezác, J., Fanfrlík, J.i., Salahub, D., Hobza, P., 2009. Semiempirical quantum chemical PM6 method augmented by dispersion and H-bonding correction terms reliably describes various types of noncovalent complexes. Journal of Chemical Theory and Computation 5, 1749-1760.

Rambousek, L., Bubenikova-Valesova, V., Kacer, P., Syslova, K., Kenney, J., Holubova, K., Najmanova, V., Zach, P., Svoboda, J., Stuchlik, A., 2011. Cellular and behavioural effects of a new steroidal inhibitor of the N-methyl-d-aspartate receptor 3α5β-pregnanolone glutamate. Neuropharmacology 61, 61-68.

Řezáč, J., Hobza, P., 2011. Advanced corrections of hydrogen bonding and dispersion for semiempirical quantum mechanical methods. Journal of Chemical Theory and Computation 8, 141-151.

Róg, T., Pasenkiewicz-Gierula, M., 2001. Cholesterol effects on the phosphatidylcholine bilayer nonpolar region: a molecular simulation study. Biophysical journal 81, 2190-2202.

Rotaru, D.C., Yoshino, H., Lewis, D.A., Ermentrout, G.B., Gonzalez-Burgos, G., 2011. Glutamate receptor subtypes mediating synaptic activation of prefrontal cortex neurons: relevance for schizophrenia. The Journal of Neuroscience 31, 142-156.

Schrodinger, L., 2015. The PyMOL Molecular Graphics System, Version 1.8, Schrodinger, LLC.

Stephens, P.J., Devlin, F.J., Chabalowski, C.F., Frisch, M.J., 1994. Ab Initio Calculation of Vibrational Absorption and Circular Dichroism Spectra Using Density Functional Force Fields. The Journal of Physical Chemistry 98, 11623-11627.

Vyklicky, V., Krausova, B., Cerny, J., Balik, A., Zapotocky, M., Novotny, M., Lichnerova, K., Smejkalova, T., Kaniakova, M., Korinek, M., 2015. Block of NMDA receptor channels by endogenous neurosteroids: implications for the agonist induced conformational states of the channel vestibule. Scientific reports 5.

Zhou, X., Ding, Q., Chen, Z., Yun, H., Wang, H., 2013. Involvement of the GluN2A and GluN2B subunits in synaptic and extrasynaptic N-methyl-d-aspartate receptor function and neuronal excitotoxicity. J Biol Chem 288, 24151-24159.